J KAU: Earth Sci., vol. 1, pp. 181-203 (1408A.H./1988A.D.)

Aerial Radioactivity of Phosphates in the Western Central Eastern Desert of Egypt

AHMED A. AMMAR[1], HASAN M. ABDELHADY[2]
SALAH A. SOLIMAN[2] and HAMDY S. SADEK[3]
[1]*Faculty of Earth Sciences, King Abdulaziz University, Jeddah, Saudi Arabia.*
[2]*Nuclear Materials Corporation, Maadi, Cairo, Egypt.*
[3]*U.S. Geological Survey Mission, Ministry of Petroleum and Mineral Resources, Jeddah, Saudi Arabia.*

ABSTRACT. Gabal Duwi Formation has been generally distinguished into lower and middle/upper phosphate-bearing members, occurring in the form of a chain along the eastern border of the River Nile between latitudes 25°10′N and 26°30′N and longitudes 32°50′E and 33°30′E for about 150 km, as well as in other sporadic locations.

Gabal Duwi Formation is characterized by intermediate to high aeroradioactivity level of anomalous nature, varying generally in radiometric intensity between 3.0 and 20.0 μR/h. The computed mean background radioactivity ranges from 4.64 to 16.5 μR/h while the standard deviation varies between 0.88 and 4.70 μR/h. These data point out that radioactivity fluctuates considerably around the calculated mean. The differentiation between the lower and the middle/upper members of the phosphate-bearing sediments appears to be possible on the basis of aeroradioactivity level which lies in the generally higher radioactivity level possessed by the latter members.

Also, it has been revealed through statistical analysis of aeroradioactivity data that the lower and middle/upper members of the Gabal Duwi Formation do not actually belong to one and the same parent population as far as radioactivity is concerned.

Introduction

The area under study, which is located to the east of Qena and Idfu cities in the western central Eastern Desert of Egypt and covers more than 8000 sq. km, lies principally between latitudes 25°10′N-26°30′N and between longitudes 32°50′E-33°30′E as shown in Fig. 1.

The purpose of this study is to map and evaluate the phosphate-bearing sediments, constituting the Gabal Duwi Formation within the area under study and occurring in the form of a chain, trending NE to Wadi Batur, NW in Wadi El Mushash and Wadi Higaza, and then due N at Gabal Abu Had, through the analysis of the recorded anomalies of increased radioactivity connected with these sediments, as the aerial

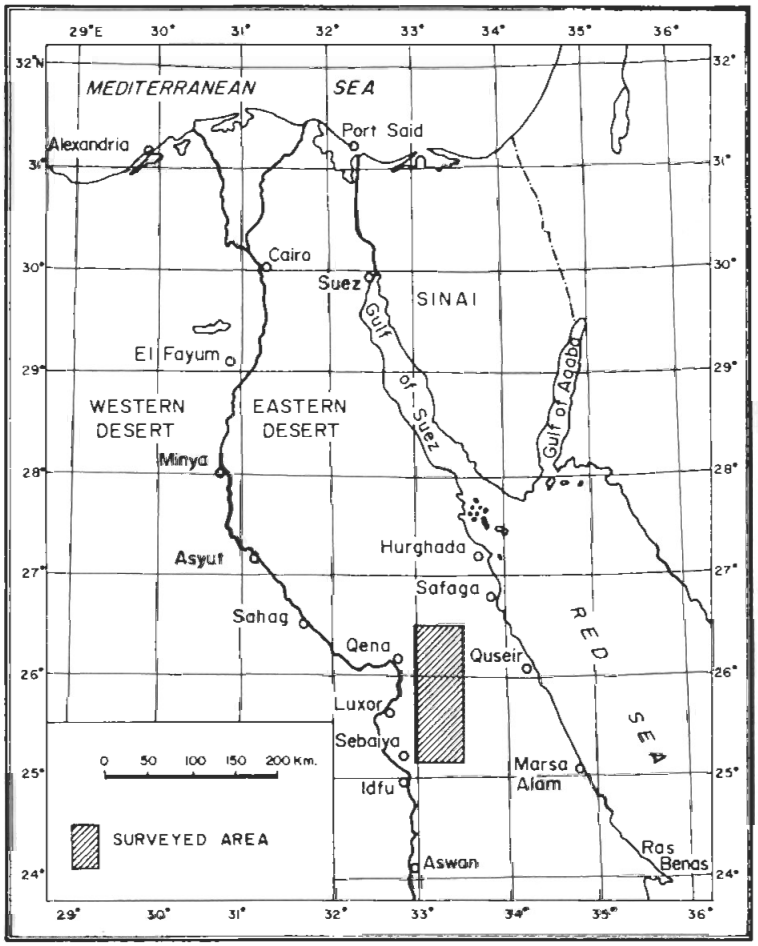

FIG. 1. A map showing the location of area studied.

radioactivity level registered over these sediments is found to be high enough – relative to the surrounding rocks possessing low to intermediate radioactivity levels – to be easily detected and mapped.

The area had been systematically surveyed by the highly-sensitived airborne radiometric apparatus (ARS-2) mounted in a maneuverable single-engine aircraft (AN-2) during the winter seasons of 1968 and 1969.

General Geology

The study of the regional geological map shown in Fig. 2 readily reveals the following:

1) The Gabal Duwi Formation, which was first defined by Youssef in 1957 to group all the phosphate-bearing sediments along the Red Sea coast, is also found by Spanderashvilli and Mansour in 1970 to include all the phospate-bearing sediments in the Nile Valley region, which are widely spreading along the eastern bank of the River Nile for more than 80 km in the latitudinal direction and over 150 km in the longitudinal direction.

2) In general, there are three different phosphate-bearing members having a total thickness ranging from 25 and 40 metres, with the lower, middle and upper members varying in thickness from 6 to 16, 6 to 15, and 3 to 12 metres, respectively (Spanderashvilli and Mansour 1970).

3) As a result of the marine invasion from the north, that followed the regression in the latest Jurassic-earliest Cretaceous, several small basins trending north-south or nearly so, almost perpendicular to the main North Egyptian Basin, were developed such as those from east to west: east Sinai, west Sinai, east Nile Delta, West Nile Delta, and four basins in the Western Desert of Egypt (El Shazly 1977).

4) The Nubian Sandstone ends with fossiliferous Senonian Sediments, including the Qoseir Variegated Shales and the El Sibaiya Phosphate Formation (Ghorab 1956, Youssef 1957, Akkad and Dardir 1966, and El Naggar 1970).

5) The marine Late Cretaceous sediments in Egypt are represented by three major facies; a phosphatic offshore facies, a basins facies, and a facies found on intervening structural highs (El Shazly 1977). The phosphatic facies occur between latitudes 25°N to 27°N, extending from El Qoseir-Safaga on the Red Sea to Qena-Idfu in the Nile Valley, and to the El Kharga-El Dakhla Oases in the Western Desert of Egypt (Hume *et al.* 1920, Ghorab 1956, Youssef 1957, El Nakkady 1958, Akkad and Dardir 1966, El Naggar 1970, Issawi *et al.* 1971, and Abdel Razek 1972).

According to Ghanem *et al.*, 1970, it was found that:

a) The principal phosphatic facies are Campanian-Maestrichtian in age, but some phosphatics occur in the Senonian. During the Campanian, the facies sequence from south to north is as follows: offshore marine and continental sands south of about latitude 24°N, offshore marine sand and clay facies which contain most of the exploitable phosphate deposits, essentially marine clayey facies between latitudes 27°N and 29°N where some phosphate deposits are present, and finally predominantly marine carbonates north of 29°N.

b) The Nubian Sandstones are overlain by a member of phosphatic bands which can be grouped into at least three horizons. Across the exposed section, three lithological bed are well-traced with full thickness of the phosphate formation reach-

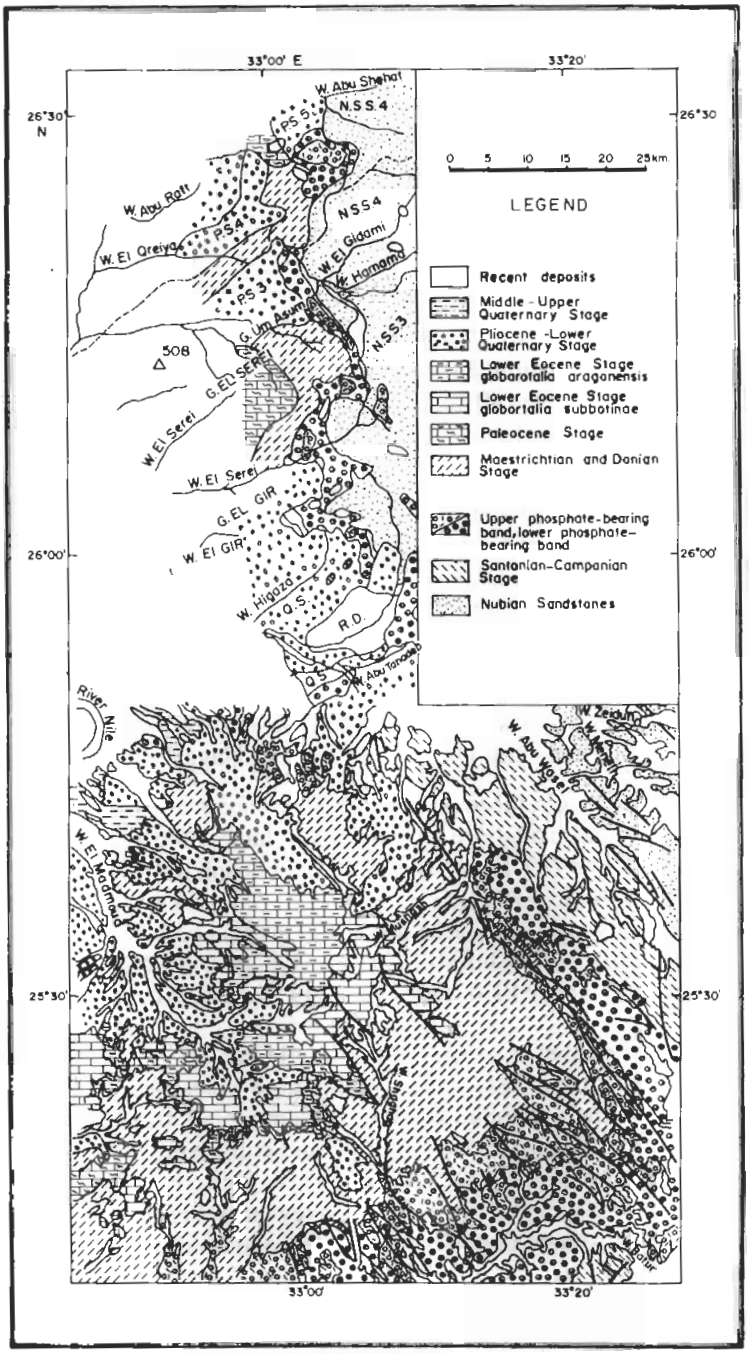

FIG. 2 Geological map of the phosphate formation, western part of the central eastern desert, Egypt (after Ghanem *et al.* 1970).

ing 90-100 metres, a lower phosphate-bearing member (4-80m), a middle phosphate-bearing member (3-10 m), and an upper phosphate-bearing member (2.5-17 m).

The lower phosphate-bearing member is an alternation of grey quartz sandstone (2-25 m) with grey and black montmorillonite beidellite clays with thickness varying from 2 to 20 m. At the base of this member, a bed of gritstone phosphate exists with a thickness varying from 0.2 to 0.6 m.

The middle phosphate-bearing member contains two main beds of phosphorites; namely, the lower bed and the middle one. The thickness of both phosphorite beds ranges from 0.5 to 1.0 m, and in places, the phosphorites are replaced by phosphatic marls or rarely by phosphatic conglomerates.

The upper phosphorite-bearing member is represented by grey carbonaceous clays, among which there is a phosphatic bed with thickness varying from 0.1 to 1.7 m, in Wadi El Mushash, and reaches 9 to 10 m in Wadi El Batur in the south.

Theoretical Considerations

Generally, all rocks and soils contain a great number of natural radioactive elements that emit gamma radiation of which the three major sources are:

a) Potassium – 40, which is 0.012% of the total potassium and emits gamma rays of an energy of 1.46 MeV;

b) Decay products in the uranium –238 and uranium –235 decay series; and

c) Decay products in the thorium –232 dacay series.

The gamma-ray spectrum from the uranium and thorium decay series is extremely complex (Darnley *et al.* 1976).

Several other sources of gamma radiation can also be detected in the field. Cosmic radiation, which is a flux of charged particles and neutrons of high energies, interacts with the atmosphere and the detectors and produces a measurable signal (Darnley *et. al.* 1976), with intensity increasing with altitude. Radioactive gases from the decay series of U-238 and Th-232 escaping into the air are also significant emitters of gamma radiation; moreover, Radon –222, because of its relatively long half-life of 3.8 days, can be transported over considerable distances in the air. For normal crustal material, most of these "background" sources of radiation represent between 5 and 15% of the total gamma radiation (Darnely *et al.* 1976).

There are three primary objectives of applications for the airborne gamma-ray surveys (Dodd *et al.* 1974):

a) To discover and evaluate large areas which may be favourable for additional exploration;

b) To locate and identify anomalies often associated with economic deposits; and

c) To support the primary geological mapping of large areas, particularly when these are difficult to access on the ground.

Survey Techniques

General Statement

The aerial radiometric survey was conducted as a series of flight lines directed northeast-southwest, with a bearing of N 60°E, oriented approximately at right angles to the main geological and structural setting of the area, to give the greatest contrast between the various geological units.

The flight was carried out at a nominal ground clearance of 70±30 metres, except under the severest conditions of relief. The average true ground speed of the aircraft during survey was about 170 km/hr. The flight line spacing was chosen to be 500 metres.

The residual background of the instrument – which represents the radiations from non geological sources and does not arise directly from the earth – was measured either at an altitude of 600-800 metres from the ground level or over the River Nile, twice every day, before and after survey (Darnley *et al.* 1979).

Instrumentation

The ARS-2 gamma radiation detection equipment used in the present aerial survey is the sensitive, quick-response instrument with continuous automatic recording of the terrestrial gamma field. The airborne scintillometer yields in flight two records: one for the total-intensity level, and the other for the hard component, instead of the altitude, in case the nature of the registered radioactivity in a discovered anomaly is to be analyzed spectrometrically. The apparatus includes the following units: cassette, amplifying and measuring unit, power pack, two-channel recording unit, and converter. The detector consists of four sodium iodide (thallium-activated) crystals, 8 cm in diameter and 5-6 cm in height.

Calibration Process

The airborne gamma-radiation metre was calibrated with the aid of standard ampoule of radium (1.02 milligram) in order to express all measurements in the generally-adopted dose-rate units, microroentgens per hour (μR/h). The results of calibration determines the sensitivity of the equipment in counts per second per one microroentgen per hour (c/s/μR/h). The standardization was periodically repeated every 7-10 working days and after repairs.

Reference graphs for the two channels of the ARS-2 instrument are shown in Fig. 3A and 3B. The sensitivity of the detector could be calculated from these graphs. It reached 173 and 4.5 c/s/μR/h for the total-count and discrimination channels respectively. The zero point is assumed to correspond to the residual background of the instrument in c/s, determined at an altitude of 600 to 800 metres above the surface of the ground.

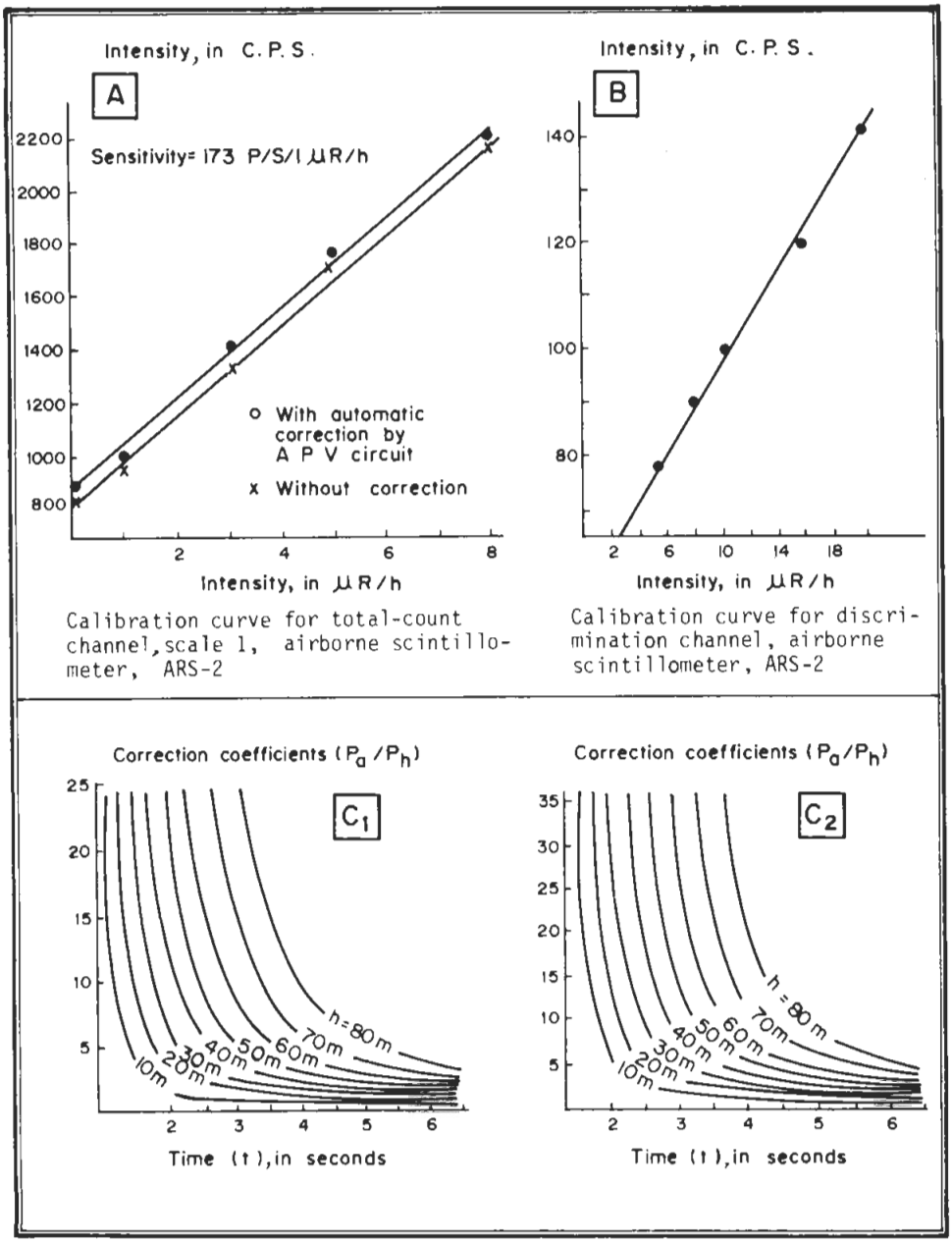

FIG. 3 Nomograms of correction coefficients (P_a/P_h) for local anomalies with preliminary recalculation by A P V – Circuit, for A R S – 2 instrument, with two time constants: $\tau_1 = 0.75$ sec. (C_1) and $\tau_2 = 1.50$ sec. (C_2) (after Nikitsky, V., 1963).

Evaluation of Local Anomalies

The anomalies are defined as any significant local increase of radioactivity exceeding the average background plus three standard deviations, *i.e.* are not due to fortuitous statistical fluctuations or chance alone.

The analysis of anomalous values were processed separately, since the measurements registered from such small-area "local" sources are undercorrected. The radiation level recorded over these point-source anomalies depends on the aircraft speed and altitude, the time constant of the instrument's integrated circuit, as well as the shape and size of the emitting surface.

An empirical nomogram, as shown in Fig. $3C_1$ and $3C_2$ (Nikitsky 1963), was used to yield the coefficient of reduction for anomalous values. This factor "P_a/P_h" depends upon the altitude "h" of the aircraft, and the time taken for recording to half anomaly amplitude, *i.e.*, duration "T". Corrections are introduced for durations less than eight seconds.

$$P_a/P_h = f(t)$$

Presentation and Analysis of the Data

General Statement

The aerial radiometric data were processed and presented in the form of aerial radiometric map, with 1.0 μR/h contour interval (Fig. 4). This map shows the various patterns and levels of radioactivity, where the isoradioactivity contour lines characterize the surface distribution of gamma activity of rocks. These patterns and levels reflect and differentiate clearly the numerous rock types and units met within the area under study, especially the phosphate-bearing sediments, through their increased and anomalous radioactivity level.

From this aerial radiometric map (Fig. 4), an interpretation unit map (Fig. 5) was prepared. The units of the last map which represent various radioactivity levels were delineated to describe various lithologic units.

The aeroradioactivity data recorded over the numerous units of the phosphate-bearing sediments were treated statistically in order to establish definite computed radiometric parameters and ranges characterizing each unit. Therefore, the measurements registered over every unit of the phosphates in the area under study – were tabulated in the form of a frequency histogram. The arithmetic mean and the standard deviation for each unit were calculated. The background was designated as all values falling within the limits of three standard deviations from the computed arithmetic mean.

The normality and/or lognormality of the distributions was carried out by both the probit transformation and the chi-square test.

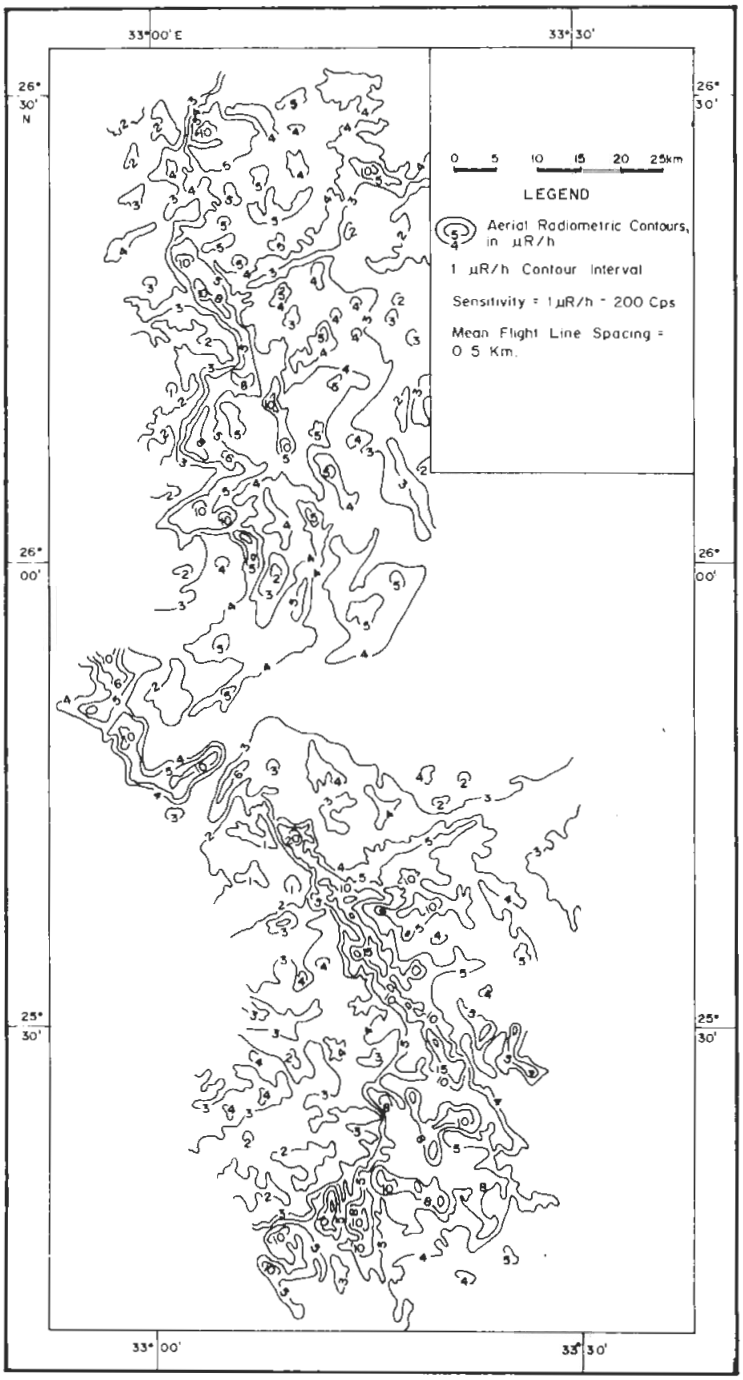

FIG. 4 Aerial radiometric map of the phosphate formation, western part of the central eastern desert, Egypt.

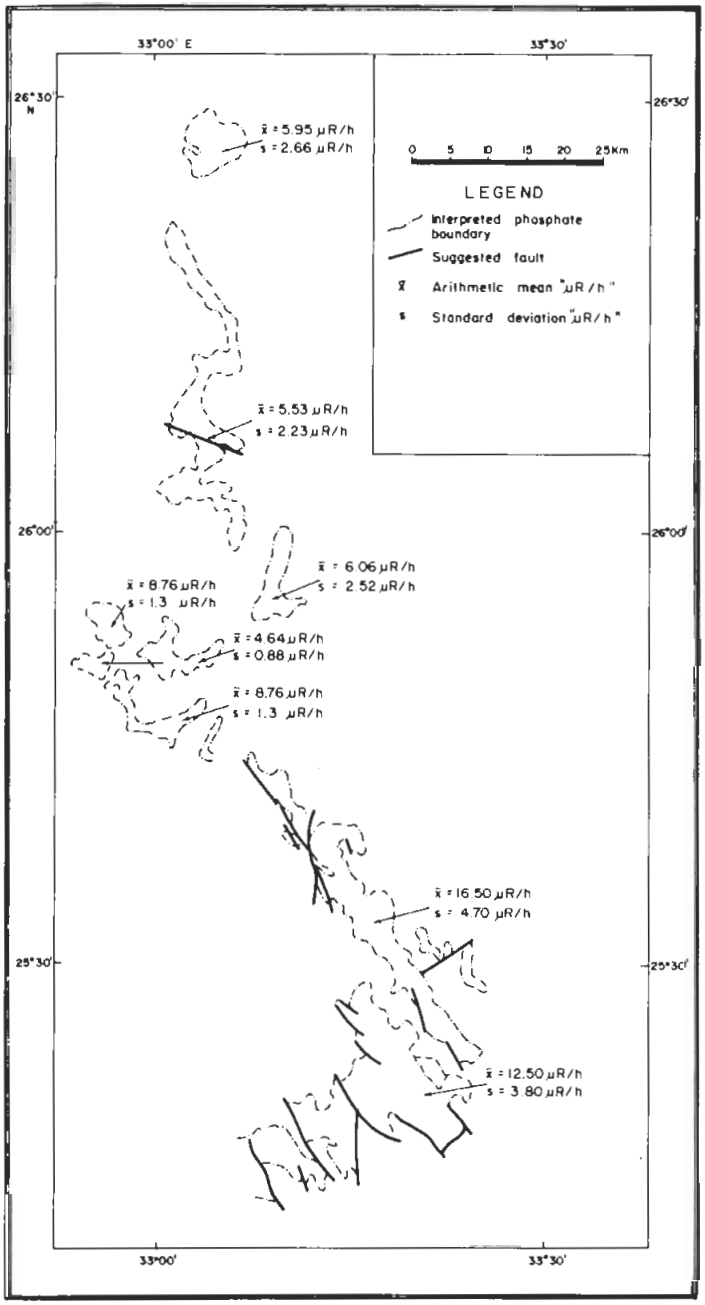

FIG. 5 Interpretation map of the phosphate formation, western part of the central eastern desert, Egypt.

Aerial Radioactivity

Phosphate-bearing sediments in the area under study may be considered as a probable source of uranium. Chemical analyses carried out in the laboratories of the Geology and Nuclear Raw Materials Department, Atomic Energy Establishment, for these deposits, have shown that the concentration of uranium in phosphates in the investigated area ranges from less than 50 to about 210 ppm. The average uranium content reached 130 ppm. The P_2O_5 content was found to vary approximately between 3 to 28 percent, while the average content reached 13.5 (Ibrahim 1974).

From the aerial radiometric map (Fig. 4), it is evident that a highly-radioactive elongated zone is present and could be easily mapped. This zone of increased radioactivity level starts from Wadi Batur and a part of Wadi Shaghab in the south trending NE-SW, then it takes the NW-SE trend making about 90° with the previous extension along Wadi Um Kharit, Wadi Mushash, and Wadi Higaza. Moreover, this highly-radioactive zone continues northwards in a N-S direction for about 50 km, to the north of Laqeita, covering Wadi El Gir, Wadi El Serei and Gabal Abu Had.

The intensity of radioactivity registered over the zone of the phosphate-bearing sediments in the area under study ranges between 5 and 25μR/h, with sharp and distinct radiometric contacts, since the surrounding rocks possess relatively much lower radioactivity levels. These radioactive anomalies of the River Nile Valley region forms a continuous zone on the aerial radiometric map (Fig. 4) in the southern parts of the investigated area, but in the northern parts, they are discrete and disconnected.

It has been proved by ground investigations that this anomalous zone of increased radioactivity is attributed to the Campanian phosphate-bearing deposits. This phophatic zone was mapped using the aeroradiometric information of figure 4 to reach to the interpretation unit map (Fig. 5). Since all the flight lines were directed perpendicularly to traverse the main extension of the phosphatic zone, *i.e.* normal to its limits or contacts, therefore, its radiometric and, hence, geologic boundaries were accurately located, traced and drawn to reach to the interpretation map (Fig. 5). This kind of mapping conforms well with the geological map of the area (Fig. 2). Consequently, more information about the occurrences of the units of the phosphate-bearing members was possible through aerial radiometric mapping. Little information about the structure of this zone could be done.

During ground investigations, at least three separate coprolite bone beds were traced. The thickness of these beds was small and did not exceed 25 cm, with an average thickness of 15 cm. In numerous localities, these beds are almost horizontal, ranging in dip from 3° to 8° to the west. They are characterized by their brecciated structure, angular bones, as well as cementation by either siliceous or carbonaceous matter. A considerable variation in grain size, hardness and colour throughout the bone beds has been noticed. The phosphate beds were seen to form the cap rock of

some plateaux, as well as the weathering products in the vicinity. These beds mainly form the phosphate-bearing sediments in the NW-SE trending exposure, while another type of phosphates is revealed in both the NE-SW and N-S trending exposures, where normal phosphate-bearing sediments exist. These normal phosphates are not resistant to weathering. Accordingly, they show very limited surface outcrops, as they are capped by another harder and more resistant kind of rocks.

The thorough examination of both figures (4 and 5) shows that the radioactive phosphate zone covering Wadi El Mushash, Wadi El Kharit and Wadi Higaza striking NW-SE possesses the highest radioactivity level compared to the remaining two phosphate zones covering Wadi El Gir, Wadi El Serei and Gabal Abu Had, striking N-S in the north of the studied area, as well as Wadi Batur and a part of Wadi Shaghab striking NE-SW in the southern part of the considered area. Moreover, the younger phosphate beds were found to possess higher radioactivity level, relative to the other more ancient beds.

Statistical Analysis

Following the radiometric mapping from the air of the phosphate-bearing sediments, into numerous interpreted units, the recorded aeroradiometric measurements were analyzed statistically. The main aims of the analysis are to help exploration for radioactive phosphates and to differentiate them into different interpreted units. The statistical analysis includes the construction of actual frequency distributions in the form of histograms, once for the readings themselves and once more for their values transformed into logarithms, especially for the not-normally distributed units. Characteristic parameters such as the arithmetic mean "$\bar{X}$", the standard deviation "S", and the background range "$X \pm 3S$" were calculated for all the distributions. The condition of normality and/or lognormality was checked by means of the probit transformation through the comparison of the empirical and fitted theoretical probits, as well as by computing the chi-square (χ^2) values through the superposition of the theoretical frequency distributions over the corresponding actual frequency histograms, at the 95% level of confidence (Dixon and Massey 1957).

The results of statistical analysis are shown in Tables (1 and 2), for the phosphatic units covering the following areas, and the enumerated as follows:

TABLE 1. Characteristic Statistics "Normal Distributions", of the Phosphate Units, West Central Eastern Desert, Egypt.

Unit No.	$\bar{X}$ μR/h	S μR/h	$\bar{X} \pm 3S$ μR/h	χ^2-Test Values		Type of Distribution
				Theor.	Calcul.	
1	10.35	2.31	17.35, 3.42	15.51	12.66	Normal
2	9.26	2.54	16.88, 2.64	15.51	11.69	Normal
3	4.64	0.89	7.29, 2.00	15.51	8.99	Normal
4	8.76	1.31	11.69, 4.83	15.51	6.21	Normal
5	6.06	2.52	13.61, –	15.51	79.68	Not Normal
6	5.53	2.32	12.48, –	15.51	44.45	Not Normal
7	5.95	2.86	14.54, –	15.51	46.57	Not Normal

TABLE 2. Characteristic Statistics "Lognormal Distributions" of the Not-Normal Phosphate Units, West Central Eastern Desert, Egypt.

Unit No.	$\bar{X}$ μR/h	Log S	$\bar{X} \pm 3S$ μR/h	χ^2-Test Values		Type of Distribution
				Theor.	Calcul.	
5	5.67	0.1827	26.38, 1.00	15.51	25.00	Not Lognormal
6	4.98	0.2208	22.89, 1.08	15.51	120.76	Not Lognormal
7	5.15	0.2365	20.04, 1.60	15.51	35.89	Not Lognormal

1. Wadi Batur and a part of Wadi Shaghab,
2. Wadi Mushash and Wadi Kharit,
3. Wadi Higaza, Lower phosphate-bearing member,
4. Wadi Higaza, Middle/Upper phosphate-bearing member,
5. East Gabal El Gir and Gabal Abu Zaalit,
6. Wadi El Serei, Wadi Um Usum and Wadi Hamama, and
7. East Gabal Abu Had and Wadi El Gir.

Concerning the southern part of the area under study, whose outcrops gave most of the high radiometric anomalies, the following two results may be reached:

1. The recorded anomalies are considered to be indications of the existence of phosphate-bearing sediments of increased uranium content. It deserves to mentioned that the phosphate outcrops striking NW-SE representing the hard and resistant varieties, possess higher radioactivity level with 200 ppm of uranium content on the average, while the NE-SW striking exposures with relatively lower radioactivity level has 40 ppm of uranium content approximately, which represent the normal type of phosphate-bearing sediments.

2. The density of the radiometric anomalies recorded from the air over the NW-SE striking exposures is heavier than that registered over the NE-SW trending occurrences of the phosphate-bearing sediments (Fig. 4). This could be explained by the fact that the phosphate beds in the first-mentioned area are more exposed than that of the last-mentioned one of the zone. If the phosphate beds are, considered to be more or less horizontal and they are, then the phosphate of the first area of the main zone could be regarded harder and more resistant than both the phosphates of the last-mentioned area of the principal zone and the overburden.

The ground investigations yielded information, which is completely in agreement with the previous interpretations. The phosphate beds of the NW-SE trending area were found to be coprolite bone beds, which are hard enough to resist wheathering and to cap most of the plateaux present in this area of the principal zone. On the other hand, the phosphates in the NE-SW striking area were found to be normal phosphates, which are soft and accordingly weathered and do not cap the plateaux. They were recognized as outcrops in stratigraphic sections, that are hidden under other more resistant beds (Sadek 1973).

Besides, at the centre of the area under study, at Wadi Higaza, the lower aeroradioactivity level connected with the lower phosphate-bearing member, could be easily related to the alternation of grey quartz sandstone with poor normal phosphates, and fragments of silicified wood. Meanwhile, the higher aeroradioactivity level related to the middle/upper phosphate-bearing member could be attributed to the coarse-grained, hard and resistant phosphate beds, and in some places to intercalations by clay beds (Abdel Hady 1973).

With reference to the northern three phosphate units, in the area under study, the differentiation between the lower and the middle/upper phosphate-bearing members on the basis of the aerial radiometric survey data seems to be a difficult process due to the relatively small thickness of the outcrops of Gabal Duwi Formation along the path of the aircraft (tenth of a kilometer in average). Hence, the records of radioactivity from the air were short and the anomalies were sharp; owing to the little time permissible for registration. These factors caused difficulties in the process of the evaluation of the anomalies, and the separation of the proper measurements related to the various phosphate members. Anyhow, the lower members of the phosphate-bearing sediments appear to be less radioactive (1.7-6.9 μR/h). Meanwhile, the middle/upper members of the phosphates may possess a higher radioactivity level (3.5-16.2 μR/h). Therefore, the phosphates could be considered possessing the highest radioactivity level with the various formations of the Foreland Sediments (Ammar 1973).

The illustrations showing the actual frequency histograms with superimposed theoretical curves, as well as the empirical and fitted probits are indicated in Fig. 6, 7 and 8.

The non-normality and non-lognormality of the three phosphate units No. 5, 6 and 7 (Tables 1 and 2) at the 95% level of significance, could be attributed to the non-homogeneity of the thickness of the phosphate beds, and also to their less competency which caused differential erosion. These results are in accordance with field observations (Ammar 1973).

Airborne spectrometry

An additional flight was conducted to investigate spectrometrically two anomalous locations of the zone of increased radioactivity level connected with the phosphate-bearing sediments of the Gabal Duwi Formation, in the area under study. The flight was carried out using an airborne gamma-ray spectrometer, type INAX, mounted in an aircraft, type Islander. The result of this survey is illustrated as a two spectrometric profiles transcribed from the actual flight, that traverse perpendicularly the phosphatic zone in two different places (Fig. 9). In this figure, the four spectrometric channels are represented: the total (T), the thorium (Th), the uranium (U) and the potassium (K). The recorded radiation in the two first-mentioned channels increase from right to left, while that of the remaining two channels increase in the reverse direction (Fig. 9).

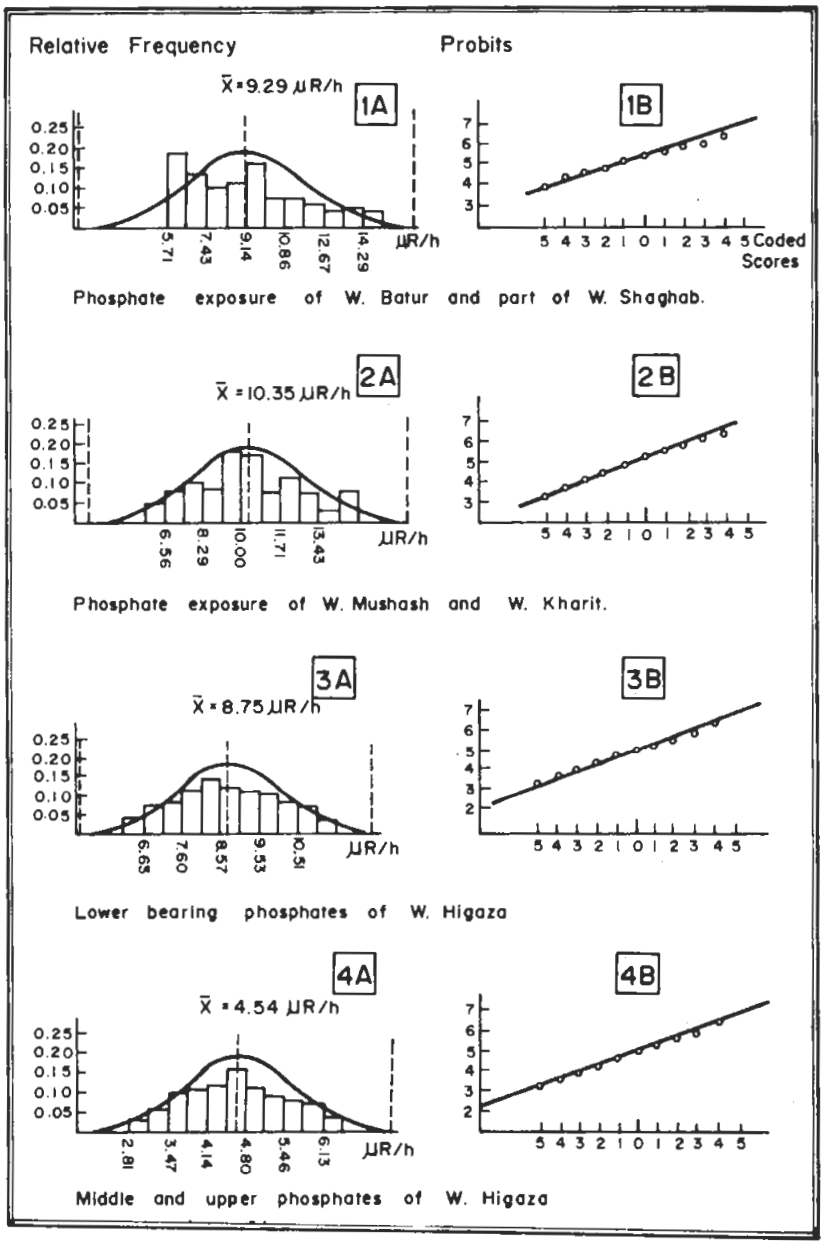

Fig. 6 Frequency histograms of the aeroradioactivity data with fitted theoretical curves (1A – 4A), and empirical probits with fitted theoretical probit lines (1B – 4B), Phosphate Formation.
W. = Wadi (Valley).

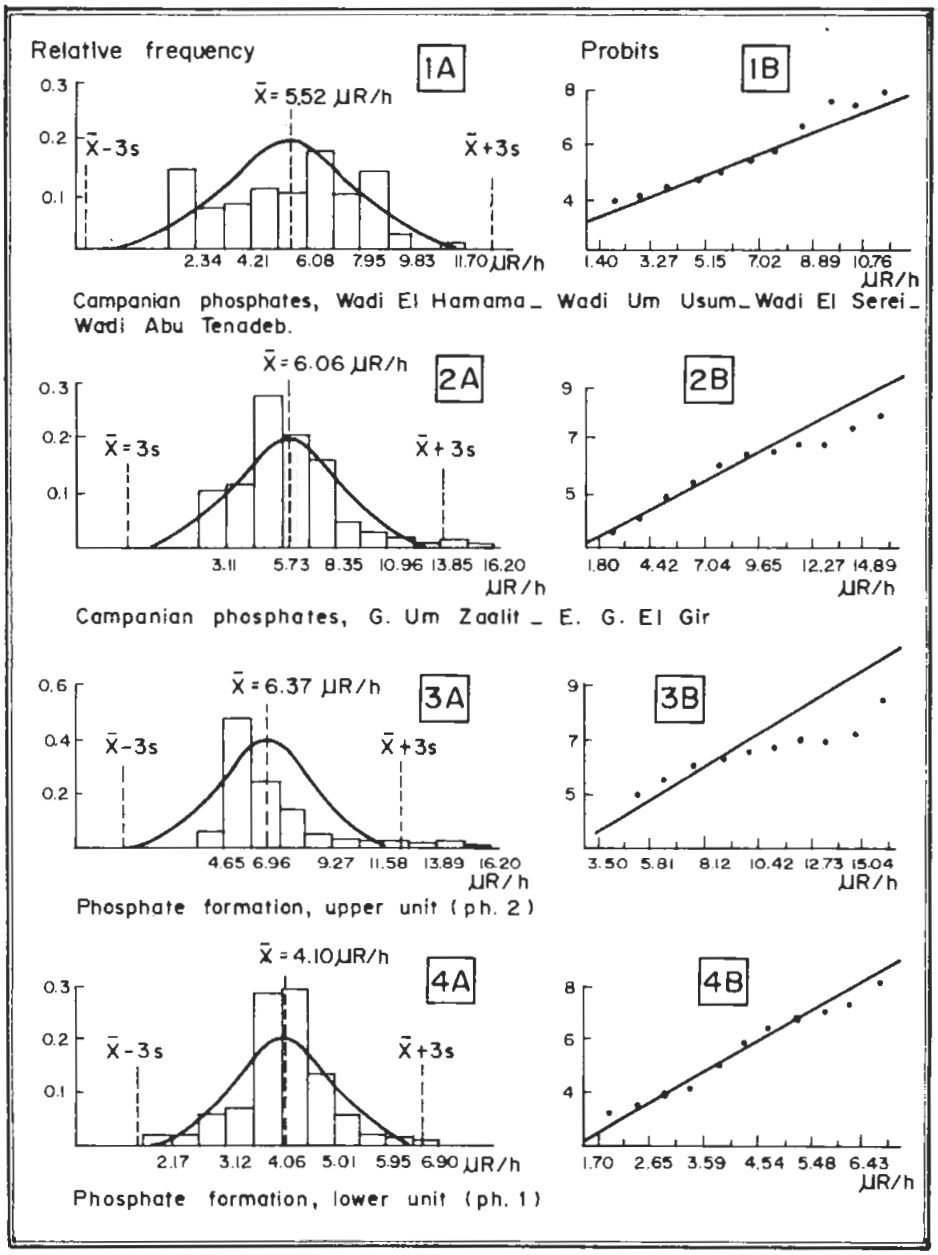

FIG. 7 Frequency histograms of the aeroradioactivity data with fitted theoretical curves (1A – 4A) and empirical probits with fitted theoretical probit lines (1B – 4B), Phosphate Formation.
G. = Gabal (Mountain).

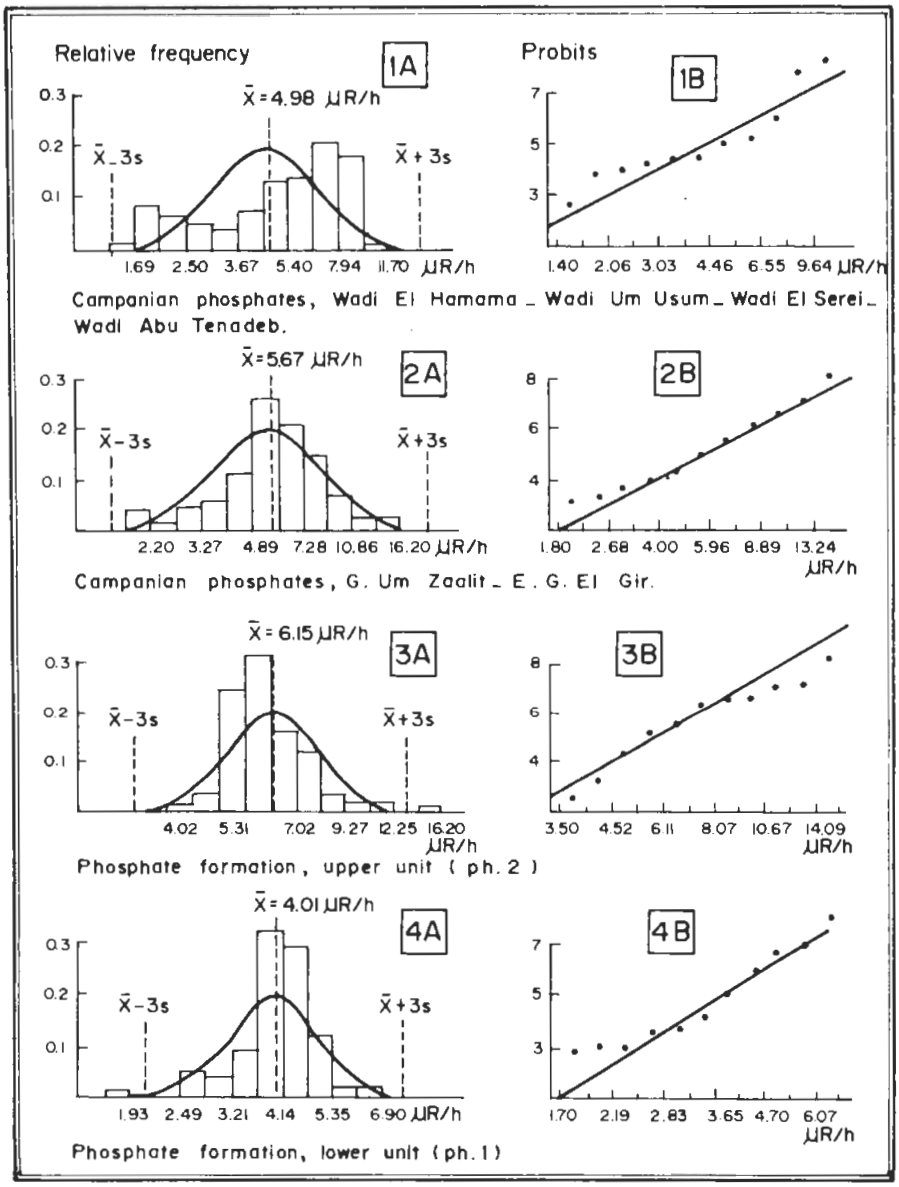

FIG. 8 Frequency histograms of the aeroradioactivity data in logarithms with fitted theoretical curves (1A – 4A) and empirical probits with fitted theoretical probit lines (1B – 4B). Phosphate Formation. G = Gabal (Mountain).

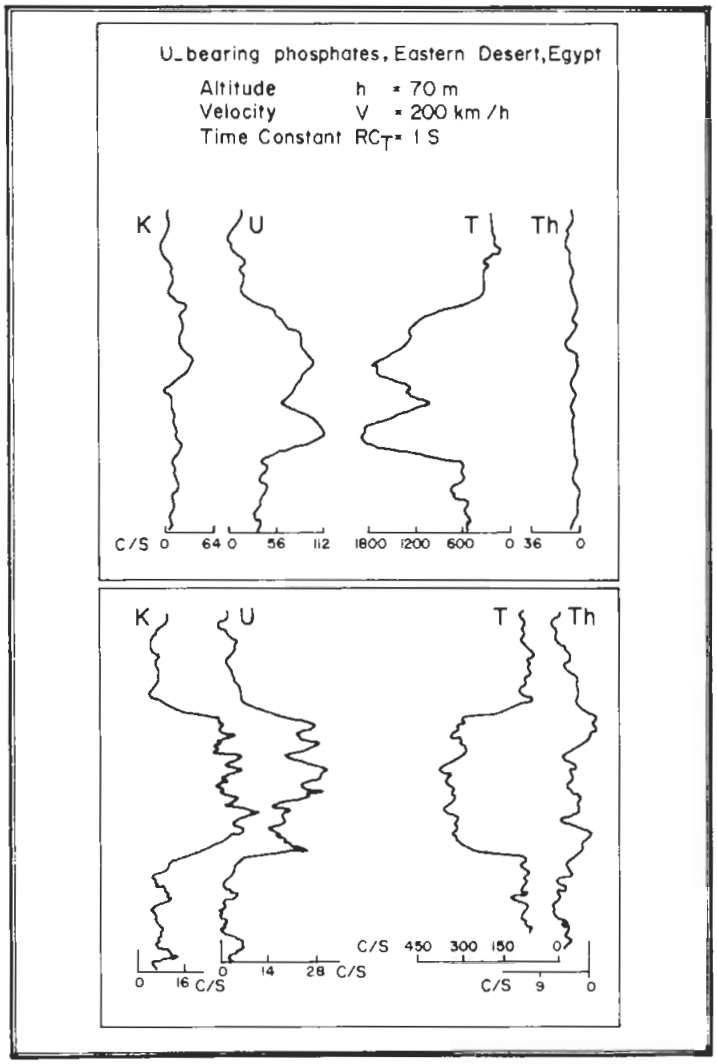

FIG. 9 Aerial spectrometric records for the 4-channels (Total, Thorium, Uranium, & Potassium), of the Airborne α-ray Spectrometer, type INAX 287-101.
Total = Total, K = Potassium, U = Uranim, Th = Thorium.

As a result of this spectrometric flight, these phosphate deposits do not contain any appreciable quantity of thorium. Meanwhile, they contain pure uranium in one of the two-surveyed locations, and a mixture of both uranium and potassium in the other place, inside the area under consideration.

Another two copies from the real radiometric record charts of the total airborne scintillation-detection equipment, type ARS-2, are shown in Figs. 10 and 11. Onto

these charts appear both the total and altitude channels, read in microroentgens/hour and metres, respectively. Both channels increase from left to right. Two examples of the method of determination of the real intensities of local radiometric anomalies resulting from the phosphate occurrences, using the nomograms illustrated in Fig. 3, are shown in Figs. 10 and 11. These two examples are introduced for comparison purposes between the results of the two instruments: the total and the spectrometric types ARS-2 and INAX, respectively.

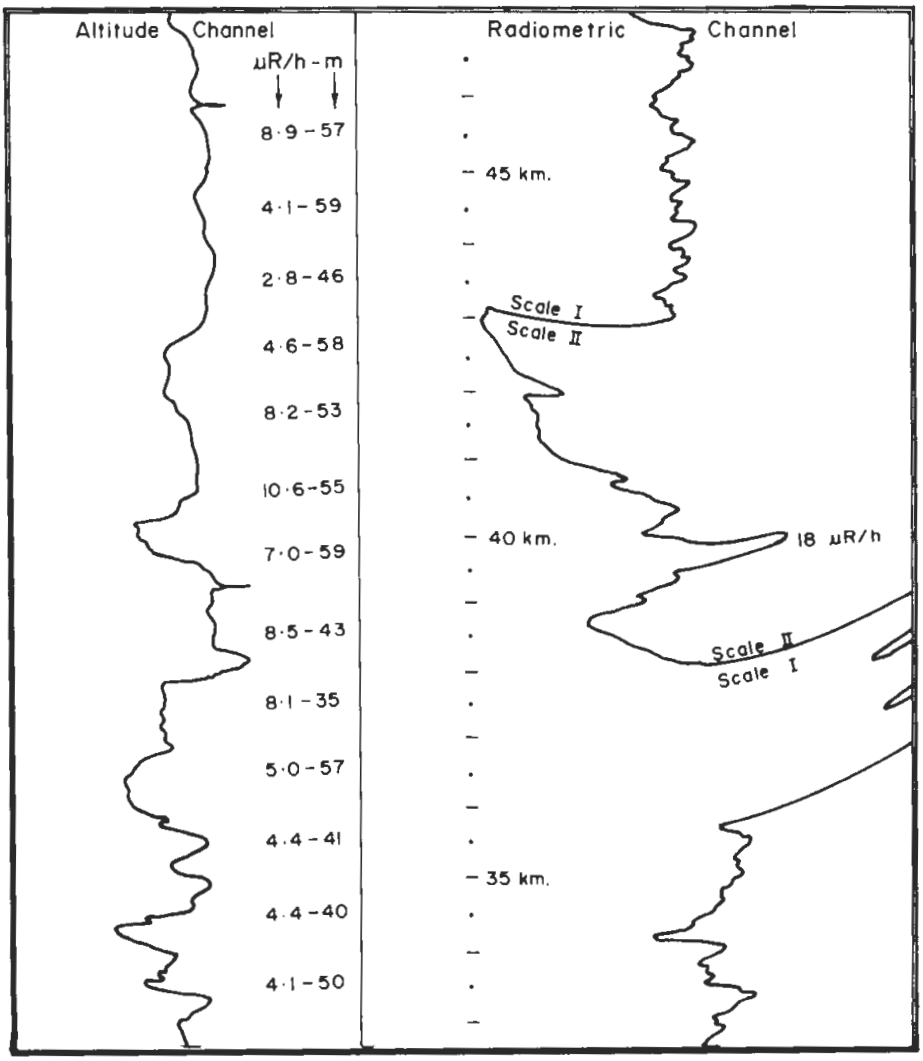

FIG. 10 An example from the record charts of the aeroradiometric anomalies of phosphates Eastern Desert, Egypt, of the total and altitude channels (in R/h and m respectively) of the airborne scintillation detection equipment, type ARS-2).

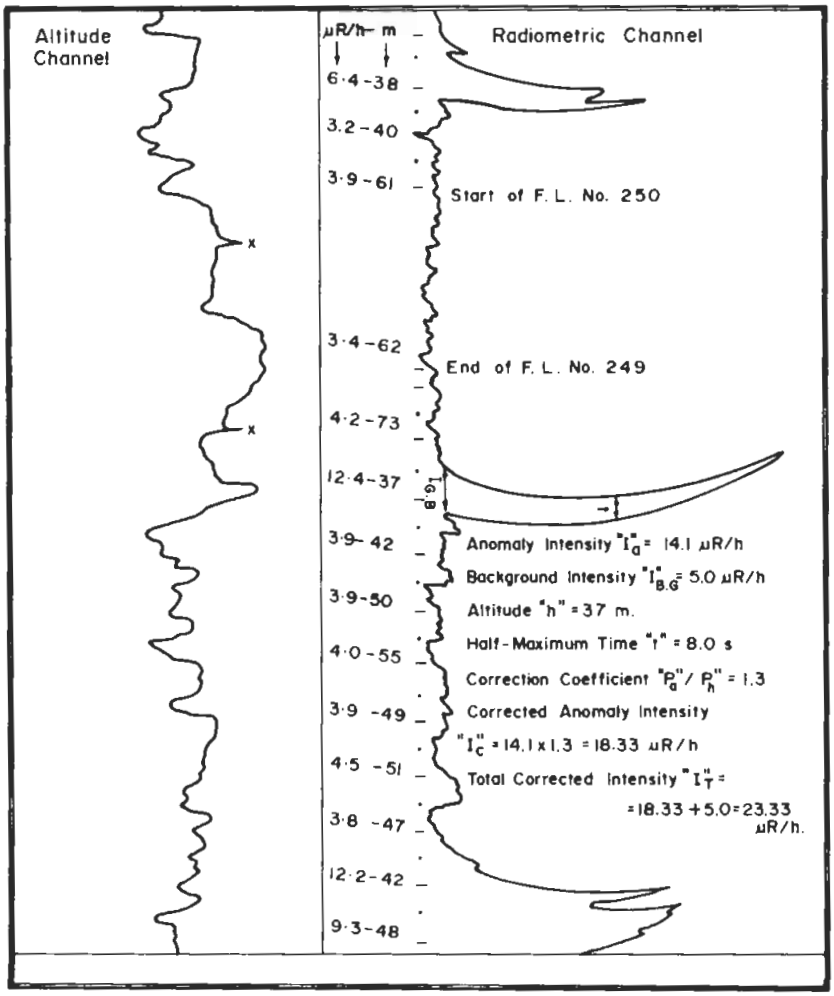

FIG. 11 An example for the evaluation of local radiometric anomalies of the phosphate-bearing sediments, Eastern Desert, Egypt, from the real record charts of the Airborne Scintillometer, type ARS-2, (the total channel on the right-hand side, read in μR/h, and the radio-altimeter channel on the left-hand side, read in metres).
F. L. No. = Flight Line Number.

Conclusions

The phosphate-bearing sediments are characterized by intermediate to high aeroradioactivity level, varying generally in intensity between 3 and 23 μR/h. The computed mean background radioactivities "arithmetic means" range from 4.64 to 10.35 μR/h, while the standard deviations oscillate between 0.88 and 2.54 μR/h, indicating that the radioactivity fluctuates considerably around the calculated mean.

The middle/upper phosphate-bearing members of the Gabal Duwi Formation appear from aerial survey to have higher radioactivity level than the lower members. It is worthy to mention that this formation possesses the highest radioactivity level ever recorded over the various groups of the Foreland Cover Sediments in the area under study.

The aerial spectrometric survey proves that the phosphates contain economic concentrations of pure uranium in some localities, which is mixed with potassium in some other places, while the thorium is absent. Accordingly, the phosphates, in the area under consideration, could be exploited for uranium as a by-product.

References

Abdel Hadi, H.M. (1973) *Interpretation of the geology of the East Luxor area in the light of the aerial radiometric mapping of Wadi Higaza area, Eastern Desert, Egypt,* M.Sc. Thesis, Cairo University, Giza, Egypt, (Unpublished).

Abdel Razek, T.M. (1972) Comparative studies on the upper Gretaccous-Early Paleogene sediments on the Red Sea coast, Nile Valley and Western Desert, Egypt. *Eighth Arab Petroleum Congress, Algiers, Paper No. 71 (B-3).*

Akkad, S. and **Dardir, A.A.** (1966) Geology and phosphate deposits of Wassif-Safaga area, *Geological Survey of Egypt, Cairo, Egypt, Paper No.* **36.**

Ammar, A.A. (1973) *Application of aerial radiometry of the study of the geology of Wadi El Gidami area, Eastern Desert, Egypt, (with aeromagnetic application),* Ph.D. Thesis, Cairo University, Giza, Egypt, 424 p, (Unpublished).

Darnley, A.G., Dodd, P.H., Duval, J.S., Lovborg, L. and **Stuart, D.C.** (1979) Gamma-ray surveys in uranium exploration, *Technical Reports Series No.* **186,** International Atomic Energy Agency, Vienna, Austria, 90 p.

Darnely, A.G., Dood, P.H., Grasty, R.L., Lovborg, L. and **Matolin, M.** (1976) Radiometric reporting methods and calibration in uranium exploration, *Technical Reports Series No.* **174,** International Atomic Energy Agency, Vienna, Austria, 57 p.

Dixon, W.J. and **Massey, F.J.** (1957) *Introduction to Statistical Analysis,* McGraw-Hill Company, Inc., New York, 488 p.

Dodd, P.H., Fabre, P., Matolin, M., Miller, J.M. and **Tolmie, R.W.** (1974) Recommended instrumentation for uranium and thorium exploration. *Technical Reports Series No.* **158,** International Atomic Energy Agency, Vienna, Austria, 93 p.

El Naggar, Z.M. (1970) On a proposed litho-stratigraphic subdivision of the Late Gretaceous-Early Paleogene succession in the Nile Valley, Egypt, U.A.R. *Seventh Arab Petroleum Congress, Kuwait, Paper No.* **64 (B-3).**

El Nakkady, S.E. (1958) Stratigraphic and petroleum geology of Egypt, *Monograph series No. 1, University of Assiut, Assiut, Egypt,* 215 p.

El Shazly, E.M. (1977) The geology of the Egyptian region, *in:* **Narin, A.E.M., Kanes, W.H.** and **Stehli, F.G. (eds.),** *The Ocean Basins and Margins,* v. 4 A, Plenum Publishing Corporation, pp. 379-444.

Ghanem, M., Mikhailov, I.A., Zalata, A.A., Pazvaliaev, A.V., Abdel Razik, T.M. and **Mirtov, Y.V.** (1970) Stratigraphy of the phosphate-bearing Cretaceous and Paleogene sediments of the Nile Valley between Idfu and Qena. *In: Studies on Some Mineral Deposits in Egypt,* Geological Survey, Cairo, Egypt, pp. 109-134.

Ghorab, M.A. (1956) A summary of a proposed rock-stratigraphic classification of the Upper Cretaceous rocks in Egypt. Presented at the *Meeting of the Geological Society of Egypt.*

Hume, W.F., Magdwick, T.G., Moon, F.W. and **Sadek, H.** (1920) Preliminary geological report on the Quseir-Safaga district, particularly the Wadi Mureikha area. *Petroleum Research Bulletin, Cairo, Egypt, Government Press,* No. **5.**

Ibrahim, A.B. (1974) *Geology, structure and radioactivity of the phosphate-bearing sediments of east Luxor area, Eastern Desert, Egypt,* Ph.D. Thesis, Faculty of Science, Ain Shams University, Cairo, Egypt (Unpublished).

Issawi, B., Francis, M., El Hinnawy, M., Mehanna, A. and **El Deftar, T.** (1971) Geology of Safaga-Quseir coastal plain and of Mohamed Rabah area, *Annual Geological Survey, Cairo, Egypt,* **1**; pp. 1-19.

Nikitsky, V. (1963) *Technichskaya instruktsia po magnitnoy razvedke,* Gosudarstvennoye Nauchno-Technicheskovoe Izdatelstvo Literaturi po Geologyi, Moskova, U.S.S.R.

Sadek, H.S. (1973) *Interpretation of the geology of east Luxor area in the light of aerial radiometric mapping, Wadi El Mushash area, Eastern Desert, Egypt.* M.Sc. Thesis, Faculty of Science, Cairo University, Giza, Egypt (Unpublished).

Spanderashvilli, G.I. and **Mansour, M.** (1970) The Egyptian phosphates. *In: Studies on Some Mineral Deposits of Egypt,* Geological Survey, Cairo, Egypt, pp. 89-106.

Youssef, M.I. (1957) Upper Cretaceous rocks in kosseir area. *Bull. Inst. Desert D'Egypte,* 7(2): 35-54.

النشاط الإشعاعي الجوي للفوسفات في غرب وسط الصحراء الشرقية بمصر

أحمد عمار[١] ، حسن عبد الهادي[٢] ،
صلاح سليمان[٢] وحمدي صادق[٣]

كلية علوم الأرض – جامعة الملك عبد العزيز بجدة – المملكة العربية السعودية[١] ، هيئة المواد النووية – المعادي – القاهرة – مصر[٢] ، بعثة المساحة الجيولوجية الأمريكية – وزارة البترول والثروة المعدنية – جدة – المملكة العربية السعودية[٣]

تم تمييز تكوين جبل ضوي – عموما إلى عضوين حاملين للفوسفات : سفلي وأوسط/علوي ، والذي يظهر على هيئة سلسلة على طول التخوم الشرقية لنهر النيل بين خطي عرض ١٠/٥٢٥ ، ٣٠/٥٢٦ شمالا ، وخطي طول ٥٠/٥٣٢ ، ٣٠/٥٣٣ شرقا ، وذلك بامتداد مايقرب من ١٥٠ كم تقريبا ، هذا بالإضافة إلى ظهوره في مواقع متفرقة أخرى .

كما أمكن تمييز تكوين جبل ضوي عن طريق مستوى نشاط إشعاعي جوي متوسط إلى مرتفع ذي طبيعة شاذة ، حيث تتغير شدة القياس الإشعاعي بصفة عامة بين ٣ ، ٢٠ ميكرورونتجن/ساعة .

وقد تراوحت خلفية الوسط الحسابي للنشاط الإشعاعي بين ٤ر٦٤ ، ١٦ر٥٠ ميكرورونتجن/ساعة ، في حين تفاوت الانحراف المعياري بين ٠ر٨٨ ، ٤ر٧٠ ميكرورونتجن/ساعة . وتشير هذه المعطيات إلى أن النشاط الإشعاعي يتذبذب إلى حد بعيد حول الوسط الحسابي . ويبدو أن التفريق بين العضوين السفلي والأوسط/العلوي من الرواسب المحملة بالفوسفات يُصبح ممكنا على أساس مستوى النشاط الاشعاعي الجوي ، والذي يكمن – على وجه العموم – في مستوى النشاط الإشعاعي الأعلى للأعضاء الأحدث .

ولقد تبين من خلال التحليل الإحصائي لمعطيات النشاط الإشعاعي الجوي أن العضوين السفلي والأوسط/العلوي لتكوين جبل ضوي لاينتميان في الواقع إلى نفس المنبع الأصلي ، وذلك بقدر مايتعلق بالنشاط الإشعاعي .